



UNIVERSITY OF
CENTRAL FLORIDA

Experimental and Numerical Evaluations of Masks and their Ability to Safely Reduce Social Distancing

Submitted to:



IAAPA

The Global Association
for the Attractions Industry

Results from:

University of Central Florida
Mechanical and Aerospace Engineering
Center for Advanced Turbomachinery & Energy Research

Principle Investigators:

Kareem Ahmed, Ph.D.
Michael Kinzel, Ph.D.

Contributing Researchers:

Jonathan Reyes, Ph.D.
Bernhard Stiehl, Ph.D.
Juanpablo Delgado
Maya Hartig
Douglas Fontes, Ph.D.

Table of Contents

Table of Contents	2
List of Figures	3
List of Tables.....	4
1 Introduction.....	5
2 Experimental Mask Evaluation	5
2.1 Abstract.....	5
2.1.1 Importance	5
2.1.2 Objective.....	5
2.1.3 DESIGN, SETTING, AND PARTICIPANTS	6
2.1.4 EXPOSURES.....	6
2.1.5 MAIN OUTCOMES AND MEASURES	6
2.1.6 RESULTS	6
2.1.7 CONCLUSIONS AND RELEVANCE.....	6
2.1.8 KEY POINTS	6
2.2 INTRODUCTION.....	7
2.3 METHODS	7
2.3.1 RESULTS	10
2.3.2 Cough Study	12
2.4 DISCUSSION	15
2.4.1 Axial distance:	15
2.4.2 Distribution characteristics:	16
2.4.3 Equivalent Distance:	16
2.5 CONCLUSION	16
3 Numerical Predictions	16
3.1 Methods	16
3.2 Results	20
3.2.1 Effect of Dampening	20
3.2.2 Effect of Filtration.....	20
3.2.3 Overall Exposure Reduction.....	22
4 Conclusions	23
5 REFERENCES.....	23

List of Figures

Figure 1: a.) Diagram of experimental set up with labeled equipment. b.) Acquisition grid used to obtain distance data.....	8
Figure 2: Path line images of compiled speech recordings a.) without a face covering b.) with a cloth covering and c.) with a three-layer mesh disposable covering.....	11
Figure 3: Path line images of compiled cough recordings a.) without a face covering b.) with a cloth covering and c.) with a three-layer mesh disposable covering.....	13
Figure 4 Schematic diagram of the physical domain.	17
Figure 5 Computational mesh used to model the respiratory function.....	19
Figure 6 Velocity at three points just outside the mouth.	20
Figure 7 Exposure as a function of radius for various particle classes. Red lines indicate no mask. Green lines indicate mask. Notice that the filtered droplets (>60 microns) virtually remain within 1ft. The aerosols, however, are substantially lower. It is important to note that the larger droplets contain the greatest volume.....	21
Figure 8 Droplet capture from the mask. This figure indicates how droplets accumulate on a mask providing a key mechanism to reduce the potentially more virulent aerosol. Note that droplets are plotted to scale with respect to other droplets, but are larger than actual. Animation can be found at: https://youtu.be/F3QWiHNOHhg	22
Figure 9 Effect of social distancing. Animation displayed here: https://youtu.be/uv__SwsyOgM	23

List of Tables

Table 1: Experiment specifications and statistical participant information.....	8
Table 2: Summarized results from all experimental test cases and participants.....	14
Table 3 Boundary conditions.	18

1 Introduction

This research surrounds social distancing. Social distancing is the strategy of reducing close contact among individuals in order to prevent the spread of pathogens and/or disease from one infected individual to another. Social distancing as an community-involved infection mitigation measure that has been put into use during arises of high contagion in the past, however the guideline of six feet for it was not actually put into effect until quite recently. In the 2009 flu pandemic, for instance, the World Health Organization (WHO) recommended an “arm’s length’ as the guideline for social distancing. The human average arm length is 25 inches, or 2.08 feet, which is notably much less than six feet.

This topic is impactful and vital to research now more than ever due to current events that have impacted the whole globe, the SARS-CoV-2 (also known as COVID-19) pandemic. SARS-CoV-2 is a respiratory disease and the prominent factor that led to its global presence is its high rate of spread that managed to pass despite government mitigation efforts around the globe. More than 112 million people have been infected with COVID-19, resulting in 2.5 million deaths and a mortality rate of 3%.²

The main source of infection transmission of the disease is via the expulsion of aerosol droplets via an infected individual coughing, sneezing, talking, or breathing, which are then inhaled by the uninfected individual.

Currently, the Center for Disease Control and Prevention, CDC, recommends the measurement baseline of six feet for social distancing. As a result, this has become the baseline measurement for social distancing all across public and commercial facilities all across the United States. However, there are contradicting research all over credible, peer-reviewed databases that suggest different baseline measurements where safety is optimal (take the aforementioned WHO 2009 recommendation, for instance). The purpose of this research is to focus on these disparities, and perform numerical quantifications to determine if the baseline for social distancing should remain at six feet, or if the safety baseline for social distancing could be satisfied with a different, lower measurement.

2 Experimental Mask Evaluation

2.1 Abstract

2.1.1 Importance

Airborne viral pathogens can be transmitted through liquid droplets/aerosols formed during human respiratory events, such as speech, cough, or sneeze. The small size of pathogens like SARS-CoV-2 enables encapsulation in liquid droplets/aerosols, increasing distances pathogens can be transmitted through airborne paths. This human research study documents and quantifies the content of droplets/aerosols at various distances without and with face coverings for respiratory events.

2.1.2 Objective

The objective of the present study is to document the propagation distance of the droplets/aerosols issued from human respiratory events (speech and cough) using face coverings.

2.1.3 DESIGN, SETTING, AND PARTICIPANTS

The number of droplets/aerosols from 1-6ft(0.305-1.829m) for cases where a host wears no face covering, a cotton cloth face covering, and a three-layer disposable face covering is measured. Investigations are conducted for a repeated defined speech pattern and cough events. The data include planar particle imagery, a technique that illuminates the emitted particles by a light sheet, and local aerosol/droplet data taken with Phase Doppler Interferometry and an Aerodynamic Particle Sizer.

2.1.4 EXPOSURES

Data collected from participants involved in the study include age, height, sex, measured droplet/aerosol sizes, and droplet/aerosol count at various distances during respiratory events.

2.1.5 MAIN OUTCOMES AND MEASURES

The primary outcome is the documentation of droplet/aerosol volume, quantity, size, and propagation distance from 1-6ft(0.305-1.829m) for a group of participants utilizing face coverings during speech and cough.

2.1.6 RESULTS

The experimental study showed a cough without any face-covering persists a maximum of 4.5ft(1.372m). Speech droplets/aerosols were detectable at a maximum of 4.1ft(1.250m). Coughing generated 1.25 times more aerosol/droplets than speech, however, they both generated similar content with a face covering. A cloth face covering reduced the maximum detectable distance of expelled aerosols/droplet to 2.22ft(0.671m), and a three-layer disposable face-covering reduced to 0.5ft(0.152m). A Z-test verified with statistical significance that physical distancing can be reduced to 1.97ft(0.600m) with a cloth covering and to 0.51ft(0.155m) with a 3-layer covering.

2.1.7 CONCLUSIONS AND RELEVANCE

The experimental study indicates that 3ft(0.914) physical distancing with face coverings is more effective at reducing aerosol/droplet exposure than 6ft(1.829m) without covering. This is relevant to physical distancing practice during the COVID-19 pandemic.

2.1.8 KEY POINTS

The formation of aerosols and droplets during human speech and cough is associated with transmitting airborne pathogens. The present experimental findings from a human research study comprised of 14 participants with age variations from 21 to 31 years, height variations of 165.1 to 185.4 cm, and a population of 79% male and 21% female. All participants are considered healthy and asymptomatic. The experiments quantify the droplet/aerosol levels at several distance with and without face coverings.

2.2 INTRODUCTION

Pandemics like the Coronavirus Disease 2019 (COVID-19) can be driven by airborne transmitted pathogens. Airborne transmission paths associated with natural human respiratory functions (speaking and coughing) are driven by pathogen-carrying droplets and aerosols^{6,7} ejected from the host and leading to various transmission paths^{8,9}. The impact of the pandemic has resulted in global-scale infection and deaths, health-system overloads, and severe economic damage¹⁻⁵. Originating from biofilms, the liquid includes multi-scales of droplets from large scales (that settle), mid scales that evaporate, and small scales (described as aerosols). The World Health Organization and the Centers for Disease Control and Prevention recommend physical distancing of 1m and 1.829m (6ft), respectively, with face coverings to reduce droplet-related pathogen transmission¹⁰.

Jennison's studies of droplets using high-speed stroboscopic light photography¹⁰ found a majority of respiratory droplets are expelled no more than 2-3ft(0.610-0.914m), with a max velocity of 152ft/s(46.33m/s), and 7-10 μ m diameter range. The study, also, qualitatively studied the effectiveness of masks. Three main parameters were found to be the main driver of filtering: material/mesh size, air permeability, and droplet permeability. The masks tested heavily reduced droplet count due to large droplets being either filtered/absorbed by the mask or subdivided by the mesh in the fabric and slowed down. The quantity and travel distance of particles after passing through the mask seemed to be based on the pressure drop across the mask. As such, the mask showed to be effective at reducing droplet/aerosol quantity and propagation distance for coughing and speaking, while being less effective against sneezes. Studies began to use this study as a recommendation for a 1 to 2-meter risk limit and that high-quality face coverings be used to further mitigate the risk of contracting an airborne infection¹¹⁻¹³.

In the present investigation, a human research study is conducted to quantify and compare the droplet/aerosol content and sizes at various distances from two respiratory events, speaking and coughing. The data are gathered using three measurement techniques simultaneously, planar particle imagery, phase doppler interferometry, and an aerodynamic particle sizer. The measurements are reported for no-face covering, a cloth face covering, and a three-layer disposable face covering. The results quantitatively verify what is reported in a recent distance study¹⁴ in the context of a group, and indicate that, with face coverings, a physical distance of 3ft(0.914m) will have less exposure to exhaled droplets/aerosols than 6ft(1.829m) without a face covering.

2.3 METHODS

Table 1 lists all equipment and participant demographics as it pertains to the study. Figure 1 depicts a schematic of the equipment's and participants' orientation relative to each other. The experiment consists of each participant reciting a phrase and simulating a cough each for 5 minutes without face-covering, with a cloth covering, and with a three-layered disposable covering. The phrase is "*The quick brown fox jumps over the lazy dog into a field of pretty playful perpetually purple pandas*". The phrase is a pangram (containing every letter of the alphabet) and has "puh", "ple", and "pra" pronunciations which create large droplets that travel longer distances¹⁰. The experiments were performed in a dust-free environment to minimize ambient particulate noise. The temperature of the room is maintained at 20°C with 35% relative humidity. The cloth face coverings (Hanes) are 3-layer, 100% moisture-wicking cotton fabric, designed to absorb incoming droplets/aerosols instead of filter and the disposable face coverings (Bailey) are 3-layer fabric with a mean pore size of 15 μ m designed to filter incoming droplets/aerosols instead of absorb.

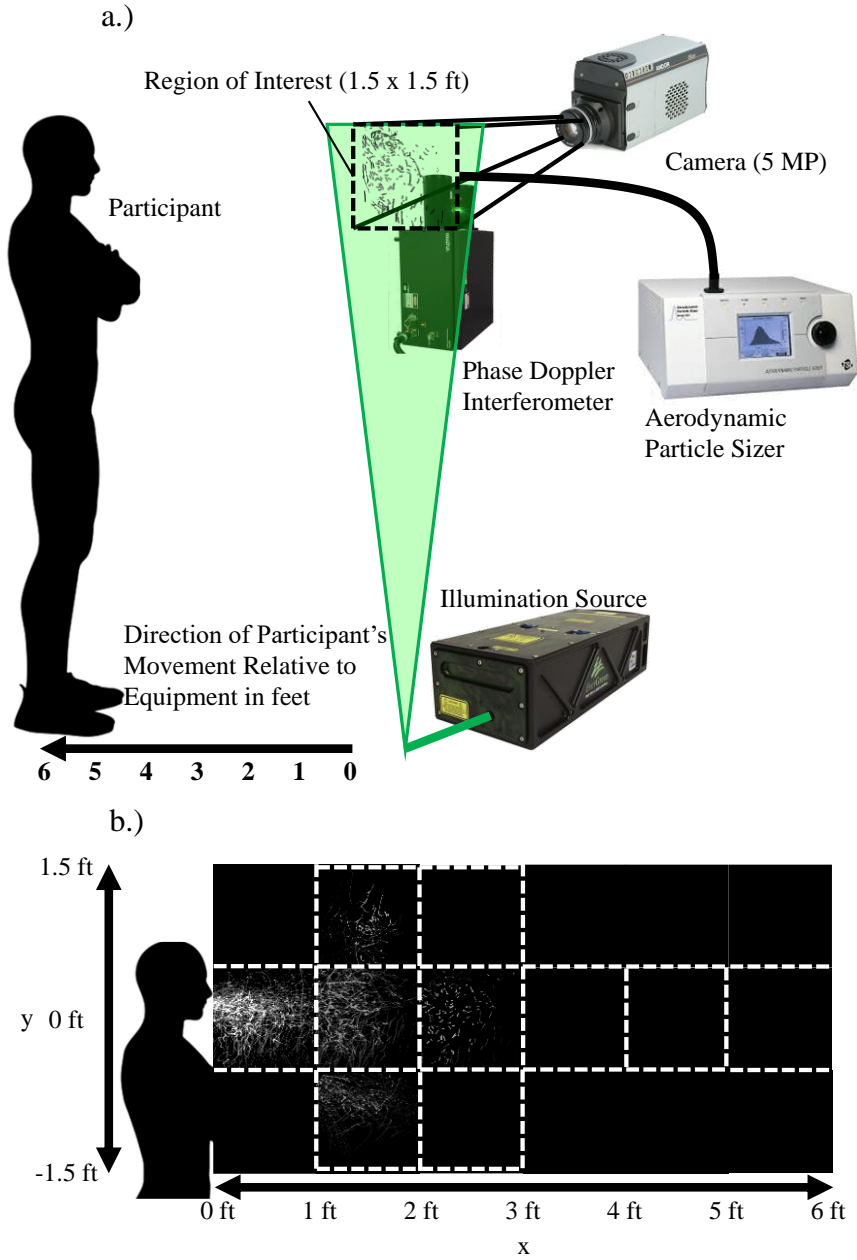


Figure 1: a.) Diagram of experimental set up with labeled equipment. b.) Acquisition grid used to obtain distance data

Table 1: Experiment specifications and statistical participant information

Equipment	Specifications	Use	Placement
Light Source	532nm, 150mJ	Particle Illumination	Region of Interest (ROI)
Camera	5MP, 30fps	Capture of Particle Scatter	5ft away from ROI
PDI	$0.5 < d < 1000\mu\text{m}$	Particle Distribution and Velocity	Region of Interest (ROI)
APS	$0.3 < d < 500\mu\text{m}$	Particle Distribution	Region of Interest (ROI)

Cloth Covering	Single Layer 100% Cotton	Exhausted Particle Reduction	Over Participant's Nose and Mouth		
3-Layer Mesh	Triple Layer 15μm mesh	Exhausted Particle Reduction	Over Participant's Nose and Mouth		
KN 95	95% Filtration for 0.3μm	Exhausted Particle Reduction	Over Participant's Nose and Mouth		
6ft Equivalent Distance (ft)					
(Buffered) [0.2 to 10μm]					
Participant (#)	Age (years)	Height (cm)	Sex	Cloth Cover	3-Layer Cover
1	28	172.7	Male	3 (±0.12)	1.5 (±0.01)
2	25	177.8	Male	3 (±0.14)	1.5 (±0.03)
3	26	170.2	Male	3 (±0.20)	1.5 (±0.01)
4	24	175.3	Male	3 (±0.11)	1.5 (±0.01)
5	23	175.3	Male	3 (±0.05)	1.5 (±0.02)
6	29	172.7	Male	3 (±0.18)	1.5 (±0.01)
7	26	165.1	Male	3 (±0.10)	1.5 (±0.03)
8	22	180.3	Male	2 (±0.02)	1.0 (±0.01)
9	30	175.3	Male	2 (±0.04)	1.0 (±0.01)
10	31	182.9	Male	3 (±0.13)	1.5 (±0.02)
11	27	185.4	Male	3 (±0.14)	1.5 (±0.03)
12	28	172.7	Female	3 (±0.13)	1.5 (±0.02)
13	27	167.6	Female	2 (±0.04)	1.5 (±0.01)
14	21	170.2	Female	3 (±0.15)	1.5 (±0.02)
Confidence in 3ft physical distancing (p-value):				0.03	0.0001
Physical Distance Equivalent for p-value of 0.05:				2.97ft(0.905m)	1.51ft(0.460m)

A high-power illumination source is used to illuminate a 1.5x1.5ft(0.457x0.457m) planar region. Aerosols/droplets entering this region produce light scatter that is captured by a 5MP camera recording at 30fps. This allows sufficient light scatter of the expelled droplets. An opaque background is used to generate greater contrast. A phase doppler interferometer (PDI, Artium Technologies 1D-PDI) and aerodynamic particle sizer (APS, Model 3321) are placed at the back center of the imaging domain (3in,7.6cm from the edge of the planar region) and are used to record the aerosol/droplet size distribution and velocity (see Figure 1a). The equipment remains stationary, and distance data is obtained by the participant moving in 1ft(0.305m) increments from the capture region.

[Figure 1 here]

There are seven marked locations for the fixed displacements each 1ft(0.305m) apart in the axial direction (see Figure 1). Data 1ft(0.305m) above and below centerline is acquired at the 1ft(0.305m) and 2ft(0.610m) locations by adjusting the equipment in the vertical direction. For speech, the participants stand at the marked location and recite the phrase for five minutes. The exhaled aerosols/droplets are illuminated and captured by the camera while simultaneously measured using the PDI and APS. Subsequently, the participant moves to the next marked location and begins reciting the phrase while data is recorded. Participants were asked to speak as loudly as possible and their decibel levels were recorded. The average decibel rating was 87.8 \pm 5.05dB.

This is repeated until the participant reaches the final location. The process is repeated with the cloth and disposable face coverings. An example of how this data is segmented and compiled is seen in Figure 1b. The experiments are repeated for a cough, with the participant simulating a cough for 5 minutes. The participants were asked to keep the rate of their coughs close to 10 coughs per minute and maintain intensity but there are some unaccounted-for variations between participants. The experiments are repeated at each location and with all types of face coverings.

The images are post-processed to create pseudo long-exposure images that represent the aerosol/droplet path lines. Generated by superimposing a two-dimensional temporal moving average at a given location from each participant and combining the locations into a particle exposure image (see Figure 1b). Aerosol/droplet loading is then calculated by normalizing the intensity of the exposure image and total counts of aerosols/droplets by the intensity and counts in the region behind the point of origin. Only 1x1ft(0.305x0.305m) of the 1.5x1.5ft(0.457x0.457m) segments are used to compile the images. This accounts for differences and movements of participants during recording and the gaussian character of the light source.

The study was designed with a power analysis to ensure sufficient participants to evaluate a hypothesis. The number of participants is based on the analysis of sample sizes for two independent samples, 3ft(0.914m)(μ_1) and 6ft(1.829m)(μ_2), assuming a continuous outcome. With a confidence level of 95% and 80% power the probabilities yield a Type I error of 5% (α) and Type II error of 20% (β). An estimated standard deviation (σ) of 3.5ft(1.067m), extracted from previous studies¹⁵, is used. In equation 1, common values for one-tail assessments of $Z_{1-\alpha/2}$ and $Z_{1-\beta}$ are used, i.e., 1.96 and 0.840, respectively. δ is 3ft ($|\mu_1 - \mu_2|$) and represents the size of the effect that is clinically worthwhile to detect. The power analysis, given as

$$N = \frac{\left(Z_{1-\frac{\alpha}{2}} + Z_{1-\beta}\right)^2 * \sigma^2}{|\mu_1 - \mu_2|^2} = 10.67 \quad (1)$$

indicates that at least 11 participants are required. In this research study, a total of 14 participants are included. The sex of the participants includes 11 males and 3 females, the heights vary from 165.1cm to 185.4cm, and participants varying from 21 to 31 years of age (see Table 1).

2.3.1 RESULTS

The results section presents the outcomes of a speech and cough study. Both studies were conducted without any face-covering, with a cloth face-covering, and with a three-layer disposable face-covering.

2.3.1.1 Speech Study

Figure 2 shows the effect of the face-covering on the distance traveled by the aerosols/droplets ejected from participants during speech. All plots in Figure 2 show time-averaged aerosol/droplet path lines from all participants. The spatial loading for each distance marker is represented by the color map and is the percentage of counted particles along the axial direction normalized by the amount at 0ft. Two-dimensional particle imagery fields and size distributions are overlaid and aligned to the axial direction. Figure 2a) is data associated with no face-covering 2b) a cloth face-covering and 2c) a three-layer disposable face-covering.

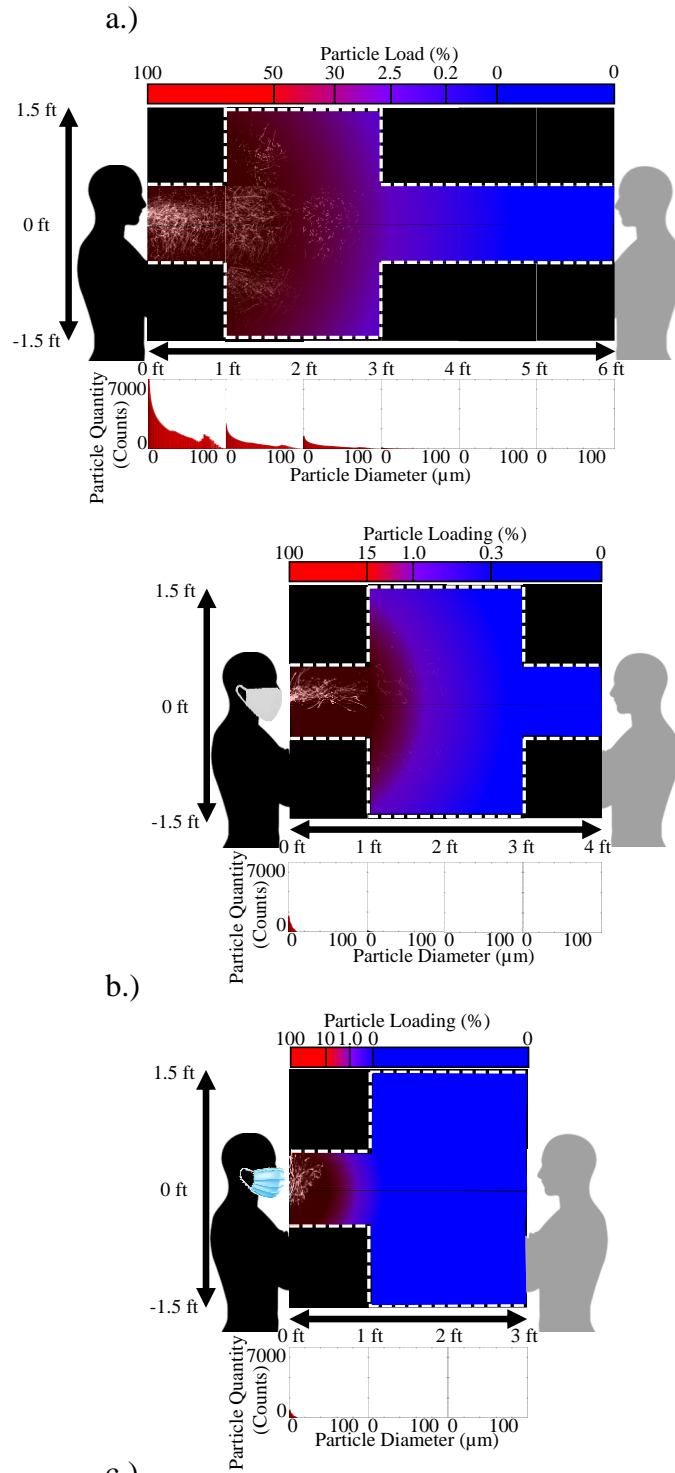


Figure 2: Path line images of compiled speech recordings a.) without a face covering b.) with a cloth covering and c.) with a three-layer mesh disposable covering

2.3.1.2 No Face Covering:

When no face covering is worn (Figure 2a), a high concentration of aerosols/droplets are visible up to 4.1ft(1.250m) downstream. Due to the limited forward momentum generated by speech, aerosols/droplets take a randomized path with little alignment to the horizontal axis. Yet, the bulk motion of aerosols/droplets remains relatively aligned to the forward direction. Maximum vertical fluctuations of $y=\pm 1.5\text{ft}(0.457\text{m})$ were recorded at an axial distance between 1ft(0.305m) and 2ft(0.610m). At 1ft(0.305 m) the PDI counted a total of 250,000 aerosols/droplets in the range of 0 to $100\mu\text{m}$, with a peak of 7,300 counts at $1\mu\text{m}$ signifying the maximum aerosol concentration. At $100\mu\text{m}$ diameter, a second peak of 1,200 droplets is measured, a local maximum that represents the larger droplet fraction. The overall measured count decreases along the axial direction, reaching 40% reduction from origin after 2ft distance, 5% after 3ft, and 0.15% after 4ft.

2.3.1.3 Cloth Face Covering:

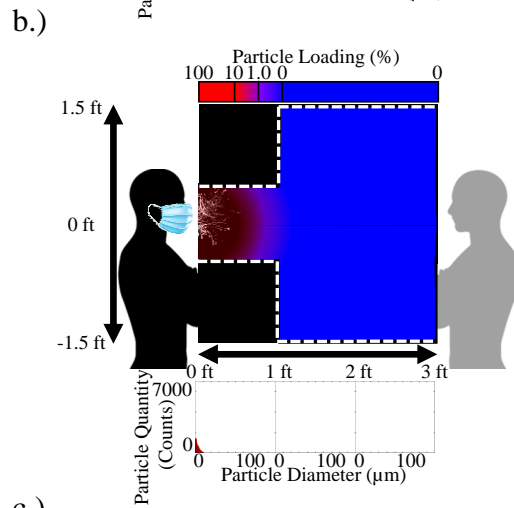
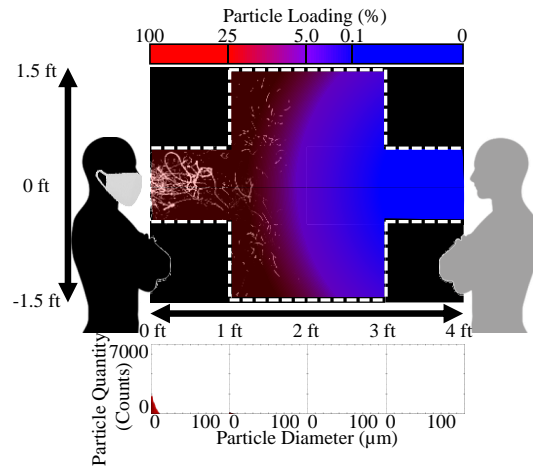
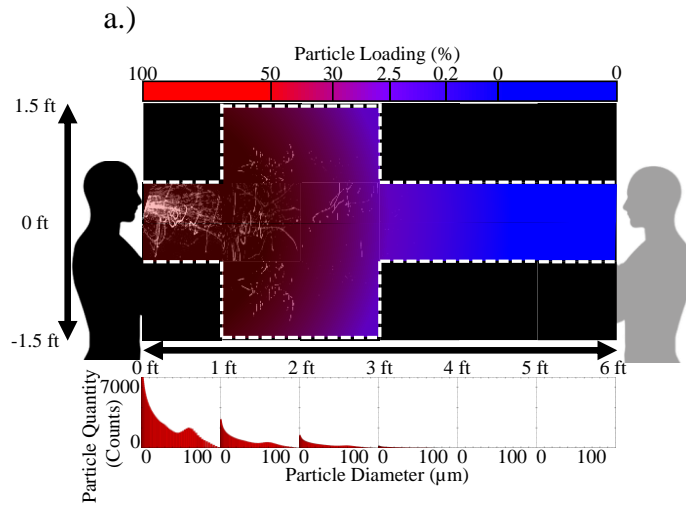
Tests with a single layered cloth face covering (Figure 2b) returned a lower number of detectable aerosols/droplets. At 1ft(0.305m), a total of 29,000 counts of aerosols/droplets were detected, a reduction of 88.4%. The large droplet fraction ($\sim 100\mu\text{m}$) was filtered entirely by the face-covering with the largest detected droplet being $21\mu\text{m}$. Approximately 1,400 units at the small scale ($\sim 1\mu\text{m}$) were able to penetrate through the face covering (a reduction of 80.8% in aerosols), leaving traces visible up to 1ft(0.305m) axial distance. Few aerosols/droplets remained detectable downstream, with total count dropping to 2,500 at the 2ft(0.610m) marker and none detected at the 3ft(0.914m) marker. The planar particle imagery data shows that at least one aerosol/droplet is present up to 2.1ft(0.64m). The use of a cloth face-covering reduces aerosol/droplet concentration and reduces propagation distance from 4ft(1.219m) to 2ft(0.610m).

2.3.1.4 Disposable Face Covering:

When a three-layer disposable face covering is worn (Figure 2c), the emission downstream of the face-covering is further reduced. Like the cloth face covering, the 3-layer covering filters out the large-scale droplets entirely. No aerosol/droplets were detected at 1ft(0.305m) and thus the PDI and APS systems were moved to 0.5ft(0.152m). At this location, a total of 15,000 counts of aerosols/droplets were recorded (a 94% reduction from without a face covering). A limited amount of about 600 units at the small-scale range ($\sim 1\mu\text{m}$) was recorded with the largest recorded droplet being $11\mu\text{m}$. From the particle planar imagery, the furthest one aerosol/droplet possibly travels is 0.5ft(0.152m). Because the three-layered disposable face-covering is not well adjustable, the images show undirected path lines originating from the chin area and from both sides at the nose. However, due to the high filtering efficiency of three-layer face coverings, horizontal emission downstream of the face covering was negligible, and reduced travel distance to 0.5ft.

2.3.2 Cough Study

The study was repeated for a series of cough events. Figure 3 is structured similarly to Figure 2, showing no face-covering in Figure 3a), cloth face covering (Figure 3b), and a three-layer disposable face covering (Figure 3c). A comparable aerosol/droplet count was recorded relative to speech¹⁰.



c.)

Figure 3: Path line images of compiled cough recordings a.) without a face covering b.) with a cloth covering and c.) with a three-layer mesh disposable covering

2.3.2.1 No Face Covering:

The cough event without face-covering yielded the maximum emission travel of 4.5ft(1.372m) per the planar particle imagery data. A cough (Figure 3) showed more aligned aerosol/droplet traces relative to speech (Figure 2). The bulk of the path lines are concentrated along the horizontal distance, traveling through the first domain with a low divergence angle of $\pm 10^\circ$. The recorded propagation shows a reduced extent in the vertical directions. Despite the focused horizontal propagation, a high concentration of falling droplets was recorded in the lower region ($y=-1.5$ ft). This was confirmed with the APS and PDI data, showing a more distinct droplet fraction relative to the speech result¹⁶. Coughing produced a total count of 300,000 aerosols/droplets (a 20% increase over speech) at the 1ft(0.305m) location with higher concentration of large-scale droplets, 2,000 counts versus 1,200 counts during speech. The large-scale droplet peak for coughing was found to be at 90 μ m, whereas speech was at 100 μ m.

2.3.2.2 Cloth Face Covering:

When coughing with a cloth face-covering (Figure 3b), a different expulsion pattern is visualized. A moderate horizontal trajectory was noticed in the first domain, yielding an approximate divergence angle of $y=\pm 45^\circ$. The vertical propagation resulted in high intensities in the outer quadrants ($y=\pm 1.5$ ft) between 1ft(0.305m) and 2ft(0.610m) axial distance. Coughing into a cloth face-covering forces aerosols/droplet to deflect due to the resistance of the mask. The expulsion exits through the crevices at the top and bottom ends of the covering, located by the nose and chin. As a result, the maximum axial penetration of one given aerosol/droplet recorded by planar particle imagery was 2.2ft in the upper and lower quadrants of the recording domain. The cloth filtered out large-scale droplets entirely with a maximum droplet diameter captured of 24 μ m. A reduction of 89.0% of total aerosols/droplets counts were recorded with 0 aerosols/droplets detectable after 2ft by the PDI and APS.

2.3.2.3 Disposable Face Covering:

Like speech, high filtering efficiency of the three-layer disposable face covering was recorded for the cough, and a propagation distance of 0.5ft axial distance is observed. The cough particles did not leave the near field of the disposable face covering. Figure 3c shows a very limited number of aerosols/droplets leave the face covering and get detected by the imaging system. The total count remained low and did not differ significantly (4% deviation) from speech.

2.3.2.4 Population Statistics:

Table 2: Summarized results from all experimental test cases and participants

Mode	Face Cover (Type)	Avg Exhausted Diameter (μ m)	Max Exhausted Distance (ft)	Avg Exhausted Velocity (m/s)	Expelled Volume(ml)
Speech	None	11.5 (± 1.1)	4.1 (± 0.25)	5.3 (± 0.32)	3.5 (± 0.29)
	Cloth	1.5 (± 0.11)	2 (± 0.13)	1.9 (± 0.14)	0.05 ($\pm 4e-3$)
	3 Layer	0.8 (± 0.06)	0.5 (± 0.04)	0.8 (± 0.05)	0.002 ($\pm 2e-4$)
	KN 95	0 (± 0.01)	0 (± 0.01)	0 (± 0.01)	0 ($\pm 1e-5$)
Cough	None	13.2 (± 1.3)	4.5 (± 0.29)	12.1 (± 0.74)	4.3 (± 0.41)

Cloth	1.9 (± 0.14)	2.2 (± 0.13)	4.8 (± 0.33)	0.07 ($\pm 5e-3$)
3 Layer	0.7 (± 0.07)	0.5 (± 0.5)	0.9 (± 0.08)	0.001 ($\pm 1e-4$)
KN 95	0 (± 0.01)	0 (± 0.01)	0 (± 0.01)	0 ($\pm 1e-5$)

Table 2 shows a list of relevant parameters that summarizes all tests and participants. To capture both aerosol/droplet size distribution and expelled quantity into a single quantity, the total expelled volume is calculated using equation 2 where V_{Total} represents the total expelled volume at the point of origin, n represents the bin number, C_n are the total counts at bin n , and d_n is the diameter of an aerosol/droplet at bin n .

$$V_{Total} = \sum_{n=1}^n C_n \frac{1}{6} \pi d_n^3 \quad (2)$$

From Table 2, speech particles are smaller than cough particles, but when either face covering is used the mean sizes are similar. Coughing propagates further than speech for the cases where no face covering or cloth face coverings were used, but the use of a three-layered face covering normalizes both events to a maximum distance of 0.5ft(0.152m). Coughing produces higher expelled velocities (~2 times that of speech) for cases with no face covering or a cloth but normalizes to less than 1m/s when a three-layered face covering is used. Coughing produces more expelled volume than speech with no face covering and the cloth face covering but are very similar in quantity when the three-layered disposable face covering is used. It is important to note the drastic reduction of over 98% in expelled volume when using either face covering. In addition, the above tests were done using a KN95 face covering, but no particles were detected for any of the participants. This could be, in part, due to the high filter efficiency of the covering (95% for 0.3 μ m and above) causing any escaped aerosols to be non-detectable by the equipment whose lowest detectable range is 0.3 μ m.

2.4 DISCUSSION

2.4.1 Axial distance:

The current recommendation for social distancing in the United States is based on the CDC guideline of 6ft(1.829m) irrespective of using face coverings and is considered safe. Findings from this study indicate that when face covering are used, equivalent 6ft(1.829m) aerosol/droplet exposure is recorded at a shorter distance. The furthest propagation measured from this study was from a cough event without any face-covering and did not travel any further than 4.5ft(1.372m) axial distance. The use of cloth face-coverings showed the ability to reduce the propagation distance to 2–2.2ft(0.610–0.671m). Additionally, the use of a three-layer disposable face-covering allowed further reduction of the axial propagation distance to 0.5ft(0.152m). The disposable face-covering performed better than the cloth face-covering due to the smaller crevices remaining further away from the mouth. No aerosols/droplets were recorded when a KN95 face covering was used for the reasons discussed prior.

2.4.2 Distribution characteristics:

Both speech and cough emission output consisted of a high-count, small diameter ($\sim 1\mu\text{m}$) aerosol fraction as well as a low-count droplet fraction at $\sim 100\mu\text{m}$ diameter without a face covering. Differences in the size and evaporation characteristics between speech and cough experiments were minor and shown to be strongly governed by the effect of the face covering, reducing the overall count by a factor of 8.7 with the cloth face covering and 16.5 with the three-layered face disposable face covering. Differences were shown with respect to the spatial distribution pattern: cough particulate showed a greater perpendicular spread and more directed particle paths, indicated by the higher exhaust velocity of the cough event. The largest amount of perpendicular ($\pm y$) effects are produced by coughing with a cloth face covering, where the cloth mask was shown to redirect the emission along a $\pm 45^\circ$ divergence angle.

2.4.3 Equivalent Distance:

Measurements indicate that with a face covering there is a reduction in expelled volume (see Table 2). The distance-dependent measurements are used to develop an exposure equivalent distance determined for each participant, reported in Table 1 for cloth and three-layer coverings (KN95 data was not detectable and thus was excluded). The exposure equivalent distance is determined by taking the total volume measured for a participant at 5ft(1.524m), and adding a 1ft(0.305m) buffer (a total of 6ft,1.829m) to ensure no exposure and finding the closest total volume equivalent when a face covering is used and adding the same buffer. The results show that the risk to emission exposure one would experience at 6ft(1.829m) from an individual without a face covering is more than what one would experience at 3ft(0.914m) with a cloth mask and nearly the same as 1.51ft(0.460m) with a three-layered disposable face covering, including buffer. A z-test was performed to evaluate if distancing can be reduced when using face coverings. The results (see Table 1) verify that there can be reduction 3ft(0.914m) with a cloth and 1.5ft(0.460m) with a three-layer covering with p-values of 0.03 and 0.0001, respectively. Additionally, we evaluated the data to identify the 6ft equivalent physical distancing (with a 95% confidence), resulting in a distancing of 2.97ft(0.905m) with a cloth and 1.510ft(0.460m) with a three-layer face covering.

2.5 CONCLUSION

The human research study of particulate propagation distance from the human respiratory events highlight, with confidence, that three feet of physical distancing with face coverings provides less risk than six feet of physical distancing without masks.

3 Numerical Predictions

3.1 Methods

Figure 1 depicts a general description of the physical setup with main dimensions of the room and human model. The physical domain consists of a representative human model placed at the middle of a room, whose length, width, and height are respectively, 10.0 m, 10.0 m, and 4.3 m. The physical domain includes inlet vent (downward arrow) flow with a weak current consistent with typical home ventilation systems of 0.39 Air Changes per Hour (ACH) with an outlet (upward arrow) to extract the air supplied from the inlet vent. Both vents are placed on the ceiling in diagonal fashion with the airflow. The main purpose of adding the ventilation is to provide: (1) conservative estimates of distance, (2) improved performance of boundary conditions, and (3) add

realism to the evaluation. Note that the vent disposition is conservative, as the current is in the same direction we are measuring droplet dispersion distance. The model of the human is an adaptation of the model developed by Fontes et al¹¹ in that it includes a person, their body, and an approximate upper respiratory tract (URT). The URT includes the pharynx, nasal cavity, buccal cavity, and teeth, which is included to provide more realistic feedback in the coupling to the mask model. The model dimensions were guided with work from Chousangsunthorn et al.¹³, however, we chose to simplify the geometry to focus on the dispersion. Key specifics include nostrils with a diameter of 0.01 m (0.4 in) and a mouth exit approximated by a rectangular shape with a width of 0.025 m (1.2 in) width and a height of 0.01 m (0.4 in). The model of the face/head was adapted from previous work to represent the human face model¹⁴. The present human body model is improved to include the mask covering the mouth and nostrils of the human model, with face contours properly fitting mask geometry with typical gaps between face and mask surfaces.

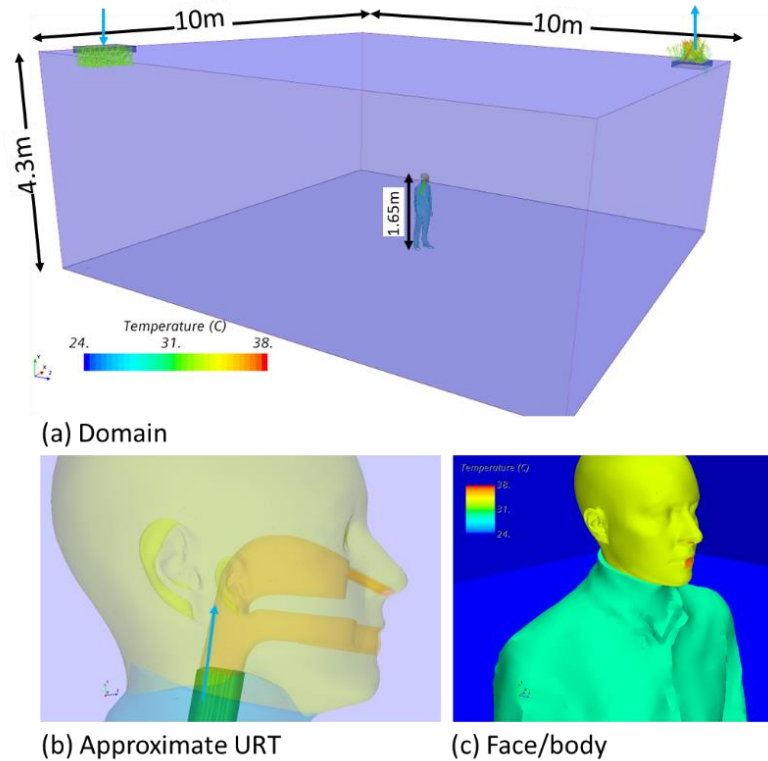


Figure 4 Schematic diagram of the physical domain.

Mass distribution of respiratory gaseous substances are tracked in this study, since the distribution of these gases has been correlated with virus transmission potential in closed rooms. Thus, the room environment consists of initially quiescent gas with the base condition, which consists of 20% of O_2 , 70% of N_2 , 5% of CO_2 , and 5% of H_2O , by mass. The air injected in the room environment during a specific respiratory event carries less oxygen and higher levels of CO_2 , modifying the gas concentration in the room with time.

The initial temperature of the room and all surfaces (walls, ground, and ceil) was kept as a constant value of 23.9 °C (75 °F). Air enters the room from the inlet vent at the same initial gas composition and temperature (base condition). Humidity, temperature, and gas composition inside the room will change according to the duration and frequency of the considered respiratory event. The outlet vent on the ceiling surface is the only outlet surface, which is defined as a constant pressure condition.

Besides the continuum representation of the air flow, the physical model considers the transport of droplets and aerosols exhaled through nostrils and mouth during respiratory events. Due to the small size of droplets associated with aerosols, smaller than 10 μm , the aerosols, mainly originated in the lower respiratory tract, are transported in the physical domain as a continuous passive scalar. The droplets, mainly formed from the mucus saliva inside the URT, are transported as Lagrangian particles. The Lagrangian droplets are submitted to drag, weight-buoyancy, shear lift, and virtual mass forces in a one-way coupling with the airflow. The droplet size changes according to evaporation/condensation and secondary breakup mechanism. The drive force for condensation/evaporation is related to the deviation of liquid-vapor equilibrium, whereas the droplet breakup is related to the ratio of aerodynamic and surface tension forces.

The gas flow coming from the bottom surface of the throat has a temperature of 37.1 $^{\circ}\text{C}$ (98.7 $^{\circ}\text{F}$) with 5% of O_2 , 70% of N_2 , 15% of CO_2 , and 10% of H_2O , slightly higher than the temperature of the internal surfaces of the throat, 36.7 $^{\circ}\text{C}$ (98 $^{\circ}\text{F}$). Around the human body model, a flow plume caused by temperature difference develops at different intensities. The human model surfaces below the neck are covered with clothes and the temperature surface was set at 29.4 $^{\circ}\text{C}$ (85 $^{\circ}\text{F}$). For the uncovered head, temperature was set at 33.3 $^{\circ}\text{C}$ (92 $^{\circ}\text{F}$).

Table 3 Boundary conditions.

Boundary	Description	Boundary value	Temperature	Species
Ceiling inlet vent	Inlet velocity	$v = 0.1 \text{ m/s}$	23.9 $^{\circ}\text{C}$ (75 $^{\circ}\text{F}$)	Base condition
Ceiling outlet vent	Pressure outlet	$p = p_{atm}$	23.9 $^{\circ}\text{C}$ (75 $^{\circ}\text{F}$)	Base condition
Walls/floor/ceiling	No slip walls	$ \vec{v} = \vec{0} \text{ m/s}$	23.9 $^{\circ}\text{C}$ (75 $^{\circ}\text{F}$)	N/A
Body: Clothes	No slip walls	$ \vec{v} = \vec{0} \text{ m/s}$	29.4 $^{\circ}\text{C}$ (85 $^{\circ}\text{F}$)	N/A
Body: Face	No slip walls	$ \vec{v} = \vec{0} \text{ m/s}$	33.3 $^{\circ}\text{C}$ (92 $^{\circ}\text{F}$)	N/A
Body: URT	No slip walls	$ \vec{v} = \vec{0} \text{ m/s}$	36.7 $^{\circ}\text{C}$ (98 $^{\circ}\text{F}$)	N/A
Body: Throat inlet	Prescribed respiratory inlet	$v = v_{breath}$	37.1 $^{\circ}\text{C}$ (98.7 $^{\circ}\text{F}$)	66.7% O_2 converted to CO_2
Body: Mask	Pressure drop	$\Delta p_{mask_{porosity}}$	$\nabla T = \vec{0}$	N/A

Regarding the boundary conditions for the Lagrangian droplets, droplets are injected from the bottom surface of the mouth of the URT. The droplets are injected at a constant volume flow rate of $10^{-3} \text{ m}^3/\text{s}$ and an injection velocity based on a normal distribution with the mean and maximum values of the normal distribution related to half and unity factors of the prescribed respiratory airflow velocity, respectively. A perfectly elastic collision is considered when the droplets hit any surface with no-slip condition. For the mask surfaces, the droplets have a conditional treatment related to the modeling of mask porosity, droplet size and velocity, as presented in the following.

The dynamic of droplets and aerosols interacting with the mask was modeled according to the droplet-permeable-wall local interaction modes. According to this model, a droplet interacting with a mask may stick to the mask surface, rebound keeping its size or breaking into smaller droplets, or penetrate the mask layers. The type of interaction is dependent on critical droplet diameter, droplet Weber, $We = \frac{\rho_f U_f^2 d_p}{\sigma_f}$, and Laplace, $La = \frac{\rho_f \sigma_f d_p}{\mu_f^2}$, numbers, and splash kinetic energy, which is a summation of incident kinetic energy, incident droplet surface energy, total

surface energy of splashing droplets, and dissipative energy loss. Here: ρ_f , μ_f , and σ_f are, respectively, the fluid density, viscosity, and surface tension; and U_I is the droplet incident normal impact velocity on the mask surface. The Weber number is the ratio between the droplet inertia and the surface energy of the droplet, while the Laplace number represents the ratio between surface tension to the momentum-transport within a fluid. The critical droplet diameter was defined based on the mask maximum pore size. Thus, droplets smaller than the critical diameter are to penetrate the mask; droplets with Weber number below the critical number, rebound; and droplets with kinetic energy below the critical kinetic splash energy will stick to the mask surface.

Similarly, to Dbouk and Drikakis (2020), the flow resistance caused by the mask during the respiratory events investigated in the present study was represented by the imposition of a pressure difference across the mask layer,

$$\frac{\Delta p}{d_f} = -D\mu_f U_f - 0.5I\rho_f |U_f|^2,$$

Where, D and I are, respectively the viscous and inertial coefficients, calculated according to the following equations

$$D = \frac{64\xi^{1.5}(1+56\xi^3)}{d_{pc}^2},$$

$$I = \frac{1}{1.28^2} \frac{1}{0.5d_f},$$

Where d_f is the face mask filter thickness, set as 2 mm.

The computational mesh is provided Figure 5. The mesh aim to directly resolve the wall boundary layers and provides appropriate, and refined, cells in the region where the respiratory events exhaust to.

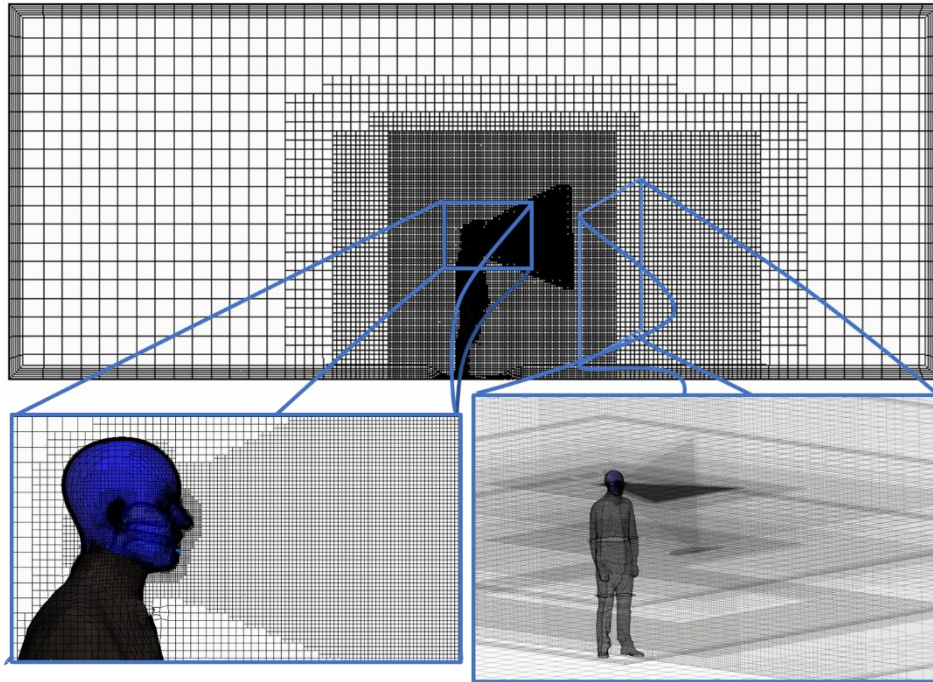


Figure 5 Computational mesh used to model the respiratory function.

3.2 Results

3.2.1 Effect of Dampening

The effectiveness of a mask is partially a result of reducing the velocity and filtering out droplets. The velocity just outside the coughers mouth, at three points, is provided in Figure 6. As the flow is driven in the model through the esophagus, novel insight is gathered into how the mask couples to the URT. What we observe is that the velocity without a mask (Figure 6a) is roughly 10 times higher than with the mask (Figure 6b). This is nothing more than the mask acting like an aerodynamic damper. However, the result is critical for mask performance as it weakens the jet that directly transports droplets to neighbors. One overall result of this is that the reduction in velocity is observed. Such a reduction enables thermal buoyancy to dominate, leading to upward/vertical aerosol transport.

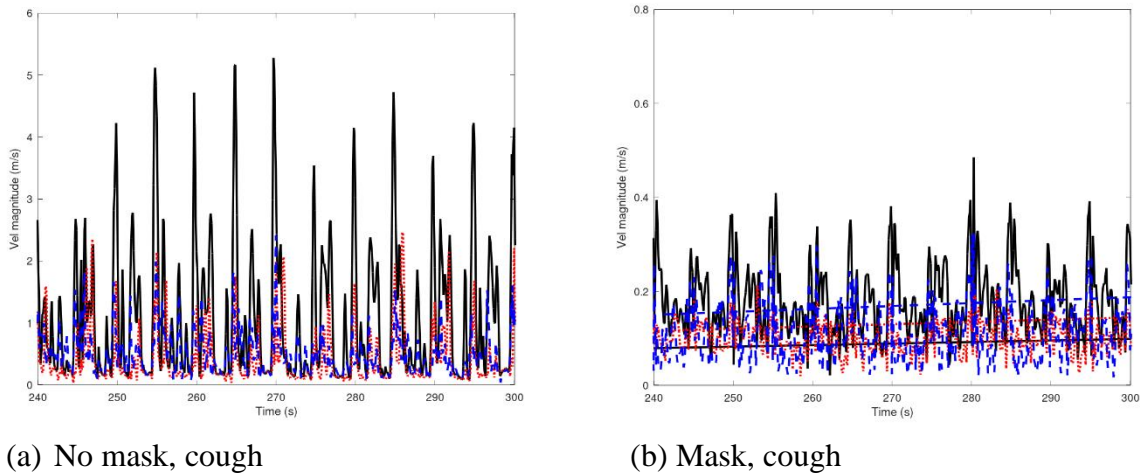


Figure 6 Velocity at three points just outside the mouth.

3.2.2 Effect of Filtration

The next aspect critical of a mask is that it filters and collects the larger droplets. It is critical to realize that larger droplets contain more fluid from the biofilms, along with the potential to aerosolize via evaporation. As evaporation implies the depletion of the liquid, and not solids, these larger droplets could have higher viral loads. In evaluating the details of the droplet and aerosol exposure at a deeper level, we can compare the exposure as a function of distance as done in Figure 7. In the figure the overall exposure (after 5 min of coughing) as a function of radius from the cougher's mouth is plotted for several droplet classes. On observation is that the mask only leads to increased exposure less than 0.5ft. At further distances, the exposure level with a mask is roughly an order of magnitude less than without a mask for all droplet classes. This implies a broad improvement in safety using the mask.

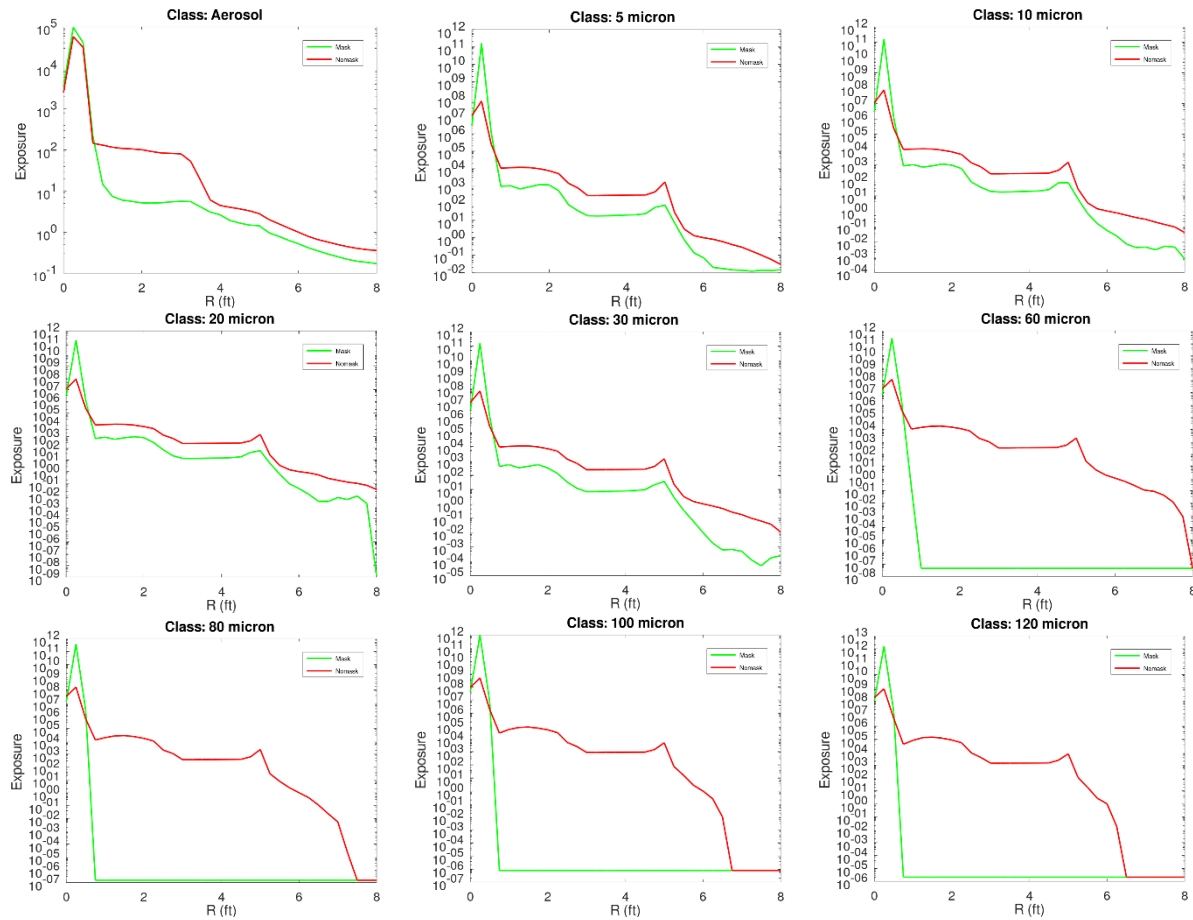


Figure 7 Exposure as a function of radius for various particle classes. Red lines indicate no mask. Green lines indicate mask. Notice that the filtered droplets (>60 microns) virtually remain within 1ft. The aerosols, however, are substantially lower. It is important to note that the larger droplets contain the greatest volume.

Additionally, insight from Figure 7 suggests that droplets over 60 microns are negligible after 1ft. The driving mechanism of this factor is the model accounting for probabilistic filtration of the droplets through the mask. Such a factor is very real and a function of the pore size of the mask. The capture of the droplets is visually represented in Figure 8, indicating droplets much larger than they actually are, however, their scale with respect to the finer droplets is representative. Note that the larger droplets are trapped in the pores of the mask, preventing the formation of a large amount of aerosols.

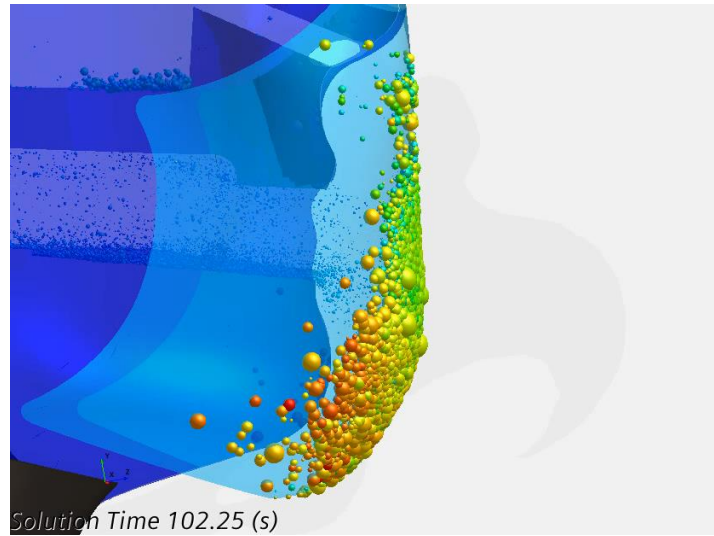


Figure 8 Droplet capture from the mask. This figure indicates how droplets accumulate on a mask providing a key mechanism to reduce the potentially more virulent aerosol. Note that droplets are plotted to scale with respect to other droplets, but are larger than actual. Animation can be found at: <https://youtu.be/F3QWiHNOHhg>

3.2.3 Overall Exposure Reduction

The impact of velocity reduction is clearly displayed in the transport of aerosols indicated in Figure 9. In the figure, is a snapshot of the darker regions that indicate a high content of exposure to aerosols. Note that with a mask, the aerosols remain in the vicinity of the cougher. Evaluating these observations, over 5 min of coughing every 5 s (i.e., 60 coughs), these exposures can be compared with respect to the guidelines from the WHO and CDC. The events highlighted in Figure 9 are peak distance events through the duration. What we can see is that the CDC provides a buffer (or safety distance) for no mask. However, when a mask is used, the buffer is more of an excess buffer, which is not practical for operation. Additionally, from Figure 7, for droplets 60-micron droplets and above, there is no apparent level of exposure beyond 1ft along with a 1 order of magnitude reduction in the smaller droplets/aerosols. Such a finding implies that practical guidelines be developed at locations where there is a sharp decline in the transport levels (i.e., in the vicinity of 1ft).

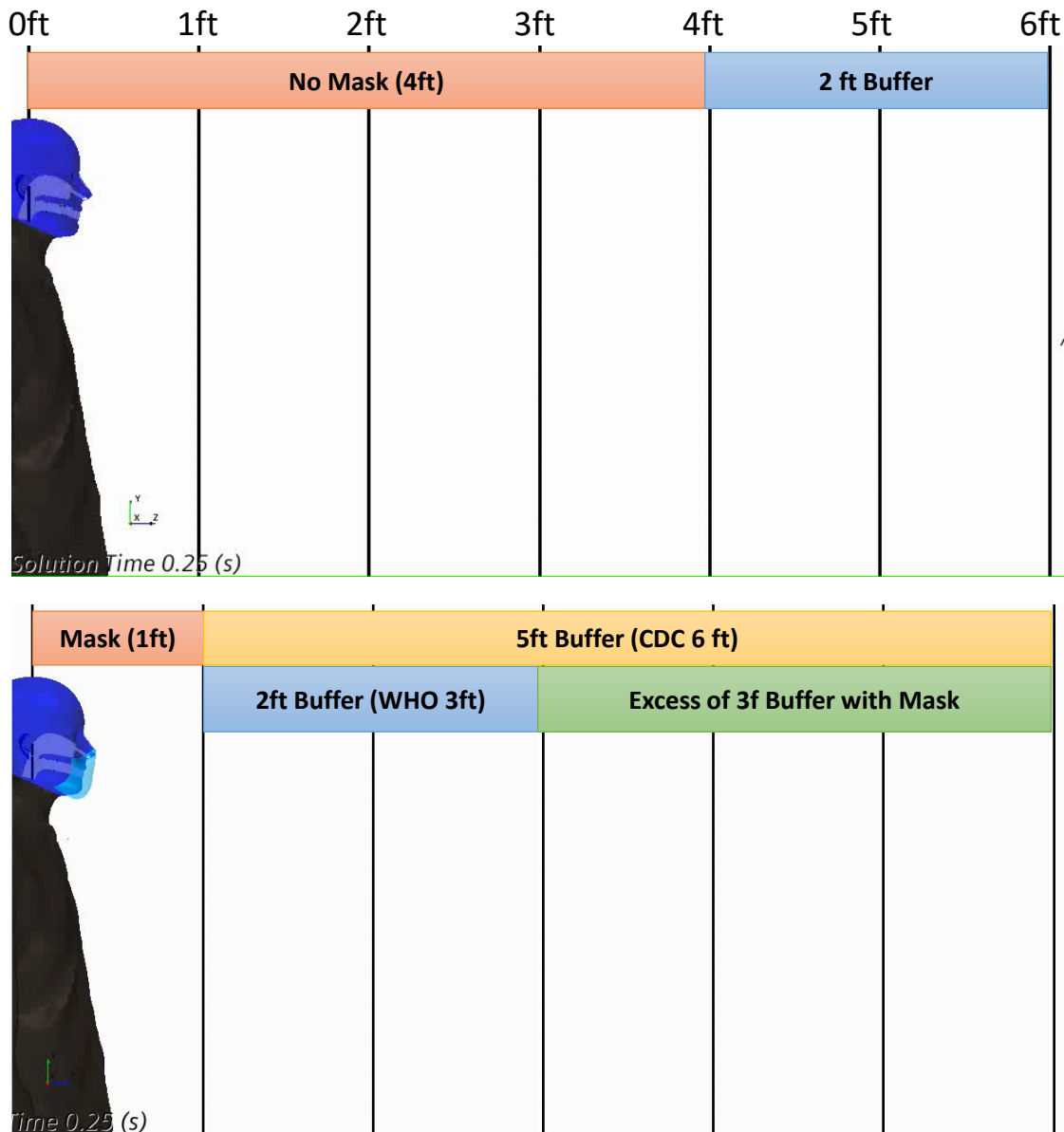


Figure 9 Effect of social distancing. Animation displayed here: https://youtu.be/uv_SwsyOgM

4 Conclusions

The experimental study indicates that 3ft(0.914) physical distancing with face coverings is more effective at reducing aerosol/droplet exposure than 6ft(1.829m) without covering. This is relevant to physical distancing practice during the COVID-19 pandemic.

The numerical results support this using high fidelity modeling. The studies specifically indicate that the effectiveness is a result of reducing velocity and filtering out the larger droplets. Additionally, these numerical results are summarized in the following you tube play list: https://youtube.com/playlist?list=PLFM_LcZ51vUyFQGscqZaoLqXq54oGWji

5 REFERENCES

1. Gupta S, Hayek SS, Wang W, et al. Factors Associated With Death in Critically Ill Patients With Coronavirus Disease 2019 in the US. *JAMA Internal Medicine*. 2020;180(11):1436-1446.

2. Richardson S, Hirsch JS, Narasimhan M, et al. Presenting Characteristics, Comorbidities, and Outcomes Among 5700 Patients Hospitalized With COVID-19 in the New York City Area. *JAMA*. 2020;323(20):2052-2059.
3. McKee M, Stuckler D. If the world fails to protect the economy, COVID-19 will damage health not just now but also in the future. *Nature Medicine*. 2020;26(5):640-642.
4. Wu JT, Leung K, Lam TTY, et al. Nowcasting epidemics of novel pathogens: lessons from COVID-19. *Nature Medicine*. 2021;27(3):388-395.
5. Carvalho T, Krammer F, Iwasaki A. The first 12 months of COVID-19: a timeline of immunological insights. *Nature Reviews Immunology*. 2021.
6. Tang J, Liebner T, Craven B, Settles G. A schlieren optical study of the human cough with and without wearing masks for aerosol infection control. *Journal of the Royal Society, Interface / the Royal Society*. 2009;6 Suppl 6:S727-736.
7. Cowling BJ, Ip DKM, Fang VJ, et al. Aerosol transmission is an important mode of influenza A virus spread. *Nature Communications*. 2013;4(1):1935.
8. Bourouiba L. Turbulent Gas Clouds and Respiratory Pathogen Emissions: Potential Implications for Reducing Transmission of COVID-19. *JAMA*. 2020;323(18):1837-1838.
9. Bourouiba L, Dehandschoewercker E, Bush John WM. Violent expiratory events: on coughing and sneezing. *Journal of Fluid Mechanics*. 2014;745:537-563.
10. Jennison MW. *Atomizing of Mouth and Nose Secretions Into the Air as Revealed by High-speed Photography*. AAAS publication no. 17 ed: American Association for the Advancement of Science; 1942.
11. Nicas M, Nazaroff WW, Hubbard A. Toward Understanding the Risk of Secondary Airborne Infection: Emission of Respirable Pathogens. *Journal of Occupational and Environmental Hygiene*. 2005;2(3):143-154.
12. Siegel JD RE, Jackson M, Chiarello L, and the Healthcare Infection Control Practices Advisory Committee. 2007 Guideline for Isolation Precautions: Preventing Transmission of Infectious Agents in Healthcare Settings. 2007.
13. Morawska L. Droplet fate in indoor environments, or can we prevent the spread of infection? *Indoor Air*. 2006;16(5):335-347.
14. van den Berg P, Schechter-Perkins EM, Jack RS, et al. Effectiveness of three versus six feet of physical distancing for controlling spread of COVID-19 among primary and secondary students and staff: A retrospective, state-wide cohort study. *Clinical Infectious Diseases*. 2021.
15. Bahl P, Doolan C, de Silva C, Chughtai AA, Bourouiba L, MacIntyre CR. Airborne or Droplet Precautions for Health Workers Treating Coronavirus Disease 2019? *The Journal of Infectious Diseases*. 2020.
16. Wells WF. On Air-borne Infection: Study II. Droplets and Droplet Nuclei. *American Journal of Epidemiology*. 1934;20(3):611-618.